informa
healthcare

Mean-Average Wall Shear Stress Measurements in the Common Carotid Artery

John N. Oshinski, PhD,[1] Jay L. Curtin, MD,[1] and Francis Loth, PhD[2]

Department of Radiology, Emory University School of Medicine, Atlanta, GA, USA[1]
Department of Mechanical and Industrial Engineering, University of Illinois at Chicago, Chicago, IL, USA[2]

ABSTRACT

In this study we determined *mean-average* wall shear stress values in the common carotid artery and assessed if there is a difference in mean-average WSS between: 1) patients with *bilateral* carotid bifurcation disease and 2) similar-aged volunteers with no evidence of disease. Sixteen patients with bilateral disease of the carotid bifurcation, and 8 volunteers were included in the study. Magnetic resonance phase velocity mapping was used to determine velocity, flow, vessel cross-sectional dimensions, and *mean-average WSS* in the common carotid artery in both the patients and volunteers. *Mean-average WSS* in the common carotid artery was 7.5 ± 2.5 dynes/cm^2 in patients and 8.0 ± 4.1 dynes/cm^2 in volunteers. There was no significant difference in *mean-average WSS,* average velocity, peak velocity, flowrate, or vessel diameter in the common carotid artery between patients and volunteers.

INTRODUCTION

Wall shear stress (WSS) is the force per unit area that blood exerts on the vessel wall in the direction of flow. WSS has been shown to affect the vessel wall at both the cellular and macroscopic level. On a cellular level, studies have shown that WSS affects the alignment, permeability, turnover rate, and adhesion of the endothelial cell layer lining the luminal surface of vessels (1, 2). WSS also mediates the production and release of a variety of vasoactive compounds by the endothelium (3–8). On a macroscopic level, atherosclerotic lesions have been shown to form in areas of low or oscillatory WSS, leading to the hypothesis that low WSS is a localizing factor for atherosclerosis

(9–11). The effects of WSS on vessels has largely been obtained through *in vitro* cellular examinations, *in vitro* studies of flow in vascular models, or in animal studies (10–13). The interest in obtaining *in-vivo* human WSS measurements has been high, but the difficulty in obtaining accurate non-invasive flow, velocity, and geometry measurements has made *in-vivo* human WSS data scarce.

In general, WSS varies with time in the cardiac cycle and circumferential position in a vessel. However, *mean-average* WSS, which is temporal *mean* over the cardiac cycle and the spatial *average* at a single axial slice location can be determined by the simple formula:

$$\tau_{\mathrm{mean-avg}} = 8\mu V_{\mathrm{avg}}/D \qquad [1]$$

where $\tau_{\mathrm{mean,avg}}$ is the mean-average WSS (dynes/cm^2), μ is the blood viscosity (cP), V_{avg} is the time-and-cross-sectional velocity average at the slice location (cm/s), and D is the diameter (cm). This equation assumes the lumen to be circular in cross-sectional shape. Mean-average WSS can be calculated easily, but there is no temporal or circumferential information about the WSS distribution.

Using ultrasound to determine blood flow velocity and vessel diameter, Gnasso et al. showed that in patients with *asymmetric* carotid artery disease (disease in one carotid but not the other), mean-verage WSS in the common carotid was higher in the

non-diseased carotid artery than in the diseased carotid artery (14, 15). The results of Gnasso et al. are interesting, but difficult to interpret since the results could imply two possible scenarios: 1) the patient had asymmetry in the level of WSS which led to the formation of disease asymmetry in the carotid bifurcation, or 2) flow was reduced asymmetrically due to increased resistance from asymmetric disease which led to asymmetric WSS. One possible way to overcome this inconsistency is to study patients with *bilateral* disease (disease in both carotid arteries). By studying patients with bilateral disease, one can determine if mean-average WSS in a group of patients which have developed atherosclerosis differs from mean-average WSS in a group of subjects which did not develop significant disease.

The purpose of this study was to determine if there is a difference in mean-average WSS in the common carotid arteries of patients with bilateral atherosclerotic disease in the carotid bifurcation and age-matched volunteers with no evidence of disease.

MATERIALS AND METHODS

Subjects

Fifty-six patients underwent magnetic resonance angiography (MRA) and phase contrast velocity mapping as well as x-ray arteriography. We retrospectively reviewed images from the subjects for the presence of bilateral carotid stenosis and inclusion in the study. All patients provided informed consent, and study protocol was reviewed by the University's Institutional Review Board. Patients underwent x-ray arteriography as part of their standard clinical assessment for carotid artery disease, and the degree of luminal narrowing was determined on the x-ray angiograms by NASCET measurement criteria (16). Twenty patients had asymmetric carotid artery disease (>50% luminal narrowing by x-ray angiography in only one carotid bulb). Ten patients did not have significant disease in either carotid bifurcation (<50% luminal narrowing by x-ray angiography in both carotid bulbs). Sixteen patients (ages 61 to 82, mean age 72 years, 8 females) had bilateral carotid artery disease (>50% luminal narrowing in both carotids) and participated in the study. No significant difference was seen between the average degree of stenosis on the left or right side when all subjects were grouped together.

The second group of study subjects was composed of eight volunteers (ages 49 to 73, mean age 63, 6 females). The volunteers were recruited from the spouses of the patients taking part in the study. The volunteers were asymptomatic for carotid artery disease, and they received both an ultrasound exam and an MRA that confirmed that they had no stenosis (0% stenosis by NACET criteria) in either carotid bulb. The ultrasound and MRA studies did not rule out wall thickening but did rule out any luminal narrowing.

MR angiography

All subjects underwent MR angiography using a two-dimensional, gradient echo, time-of-flight (TOF) sequence. Transverse slices were acquired perpendicular to the carotid

Figure 1. Maximum intensity projection (MIP) image created from a series of transverse MR time-of-flight (TOF) images of the right carotid artery of a volunteer. The line indicates the location of the slice for the phase velocity measurement.

artery from approximately 3 cm below the bifurcation to approximately 3 cm above the bifurcation. The sequence has been described in detail elsewhere (17). Briefly, the imaging field-of-view (FOV) was 160 mm, scan matrix was 256 × 256, flip angle was 60 degrees, TR was 9–18 msec, and TE was 4–6 msec. All scans were done on a Philips Medical Systems 1.5 Tesla ACS-NT scanner (Philips Medical Systems North America, Shelton, CT, USA). Anteroposterior (coronal) and lateral (sagittal) maximum intensity projection (MIP) images of each artery were reconstructed from the transverse slices which allowed determination of the location of the carotid bifurcation (Fig. 1).

MR velocity measurements

Velocity measurements were made with a slice positioned in the common carotid artery 1 cm below the carotid bifurcation. The slice was positioned perpendicular to the common carotid artery on both the MIP images (Fig. 1). Velocity measurements in the foot-head direction were made using a phase velocity mapping sequence. The sequence acquired interleaved velocity compensated and non-compensated phase images that were subtracted to yield a phase map in which velocity was proportional

J. N. Oshinski et al.

to the phase shift of the MR signal. Phase shift was converted to a velocity value, and the velocity values were displayed as grayscale image intensity. Details on the technique have been presented elsewhere, and several studies have used the technique to measure velocities both *in vitro* and *in vivo* and have shown accuracy and reproducibility to be 2–5% (18–20).

The velocity encoding value was set such that a phase shift of π radians corresponded to a velocity of 50 cm/s and velocity was encoded in the slice-select direction only. Field of view was 160 mm with an acquisition matrix of 256×256, giving an approximate pixel resolution of 0.6×0.6 mm. Slice thickness was 5.0 mm, and the head coil was used for all imaging. The flip angle was $35°$, the repetition time (TR) was 14 msec, the echo time was 8 msec, and two signal averages were acquired for each scan. Retrospective cardiac gating was used, and 16 images equally-spaced over the cardiac cycle were reconstructed, the first phase being 8 msec after the R wave.

Phase velocity image analysis

All analysis of the phase velocity data was done on the program FLOW (AZL, Leiden, The Netherlands) (21). The average cross-sectional velocity at each time point was determined for each patient by averaging all velocity values within the user-traced boundary around the vessel. To determine flow over the cardiac cycle, the phase velocity maps were integrated on a pixel by pixel basis within a user traced boundary of the carotid artery.

The diameter of the carotid artery was measured at systole and diastole by taking the average of an anterior-posterior diameter and a left-right diameter on the magnitude images corresponding to the phase maps. The systolic image was identified as the image where flow was maximum, and the diastolic image was the last image before the R-wave. Average vessel diameter was defined as the average of all four measurements of diameter.

The time-average, mean cross-sectional velocity (cm/s), peak velocity (cm/s), flow over the cardiac cycle (mL/min), systolic diameter (cm), diastolic diameter (cm) were determined for each subject. Differences between the patients and volunteers were assessed with a t-test.

Determination of wall shear stress

Mean-average WSS was determined by equation 1 for each subject. The mean-average WSS is both the temporal mean value of WSS over the cardiac cycle and the spatial average around the circumference of the vessel at the point where phase velocity measurements were made (one centimeter below the carotid bifurcation). Since blood samples were not available on the patients or volunteers, a blood viscosity value of 4.0 cPoise was assumed for all subjects (22). Differences in mean-average WSS between the patients and volunteers were assessed with a t-test. A power analysis and sample size test were performed. The number of subjects in this study was adequate to see a difference in WSS of 3.0 dynes/cm^2 between the two groups with a power of 90% (23).

Equation 1 is valid for fully developed pulsatile flow in a straight, rigid vessel of circular cross-section. Under these as-sumptions, the Navier Stokes equation is linear in time, and hence, obeys the principle of superposition. Therefore, the pressure gradient driving the flow can be represented as the sum of its mean and oscillatory components, and the WSS can be computed by the sum of solutions for each pressure gradient component (24). The mean of the oscillatory components of WSS is zero; hence, the only contribution to the *mean* WSS is from the *mean* pressure gradient. The *mean* pressure gradient corresponds to the *mean* (steady flow) formula for WSS (eq. 1). Although the common carotid artery is not a rigid, straight tube, in most patients, there is a fairly long section of vessel before the bifurcation to allow axial flow development. Vessel compliance has been shown to be a secondary effect in WSS (34).

Peak WSS could be determined by replacing the mean velocity with the peak velocity in eq. 1. However, this requires an assumption of a parabolic velocity profile at peak flow, which is not required for the calculation of mean WSS. Peak systolic flow is often not fully-developed and hence would not have a parabolic profile. Calculation of peak WSS by using peak velocity in equation 1 will result in underestimation of peak WSS. Hence, peak WSS was not evaluated in this study.

RESULTS

MR velocity measurements

The MR phase velocity mapping sequence produced images with sufficient signal to noise and resolution to calculate velocities, flowrates, diameters, and WSS in all subjects. A typical phase velocity map is shown in Fig. 2. On the phase map, bright vessels represent arterial flow toward the head, while the dark vessels represent venous flow toward the feet. Mid-grayscale
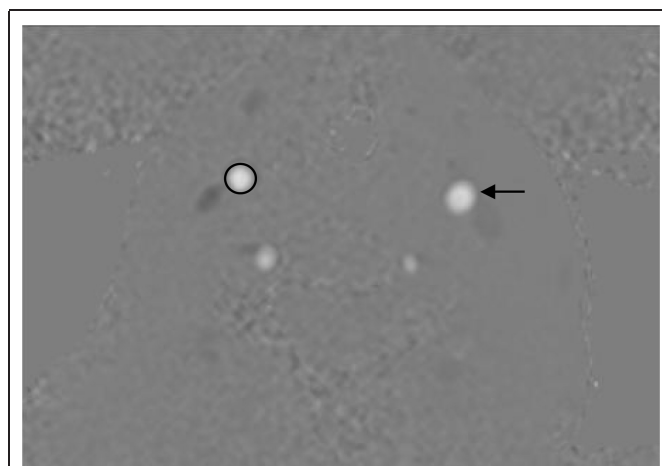
Figure 2. Peak systolic phase image from the common carotid artery (CCA) in one of the volunteers. Bright signal indicates flow toward the head (arteries) and the dark signal indicates flow toward the feet (veins). The arrow points to the left CCA, and a user drawn region of interest (ROI) around the CCA is shown on the right CCA. The ROI is propagated over all cardiac phases to determine the area, flow, average and peak velocity.
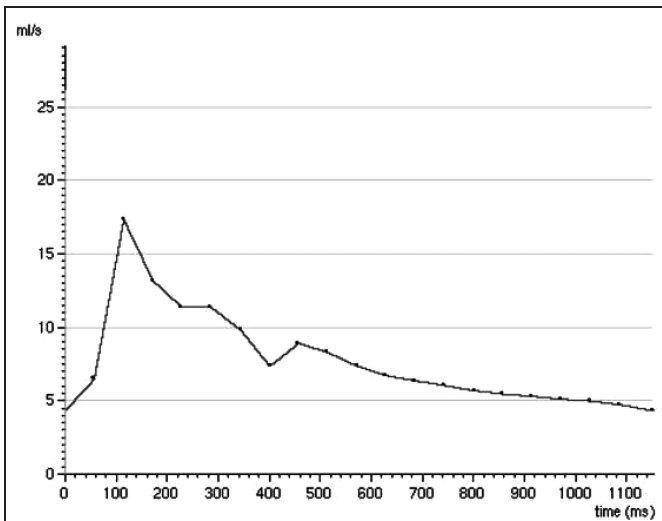
Figure 3. Flow curve (flow in ml/sec versus time in the cardiac cycle) from a volunteer. The flow waveform is typical of carotid arteries. There is some pulsatility, but no periods of zero flow, due to the low resistance of the cerebral vasculature. Flow pulsatility in the patient was lower than in the volunteer, presumably due to the increased resistance to flow in the stenosis or due to changes in the vascular compliance.

regions represent zero-velocity areas of static tissue in which no appreciable fluid flow occurs.

The phase maps at the 16 time points over the cardiac cycle were integrated over the carotid artery cross-section to yield curves of flow versus time for each subject. A typical flow curve from a subject is shown in Fig. 3. None of the patients or volunteers showed reverse flow in the common carotid artery during the cardiac cycle. This absence of reverse flow is consistent with the low resistance of the cerebral vasculature. Although not quantitatively assessed, the flow in the volunteers generally appeared to be more pulsatile than flow in the patients. This was expected, as the increase in flow resistance caused by stenoses will decrease flow pulsatility (25, 26).

Temporally and spatially averaged velocity measurements, flow measurements, peak velocity measurements, vessel diameters at systole and diastole, and ages for each group of subjects

Table 1. Values for diameter, velocity, flow and wall shear stress summarized for the patients and volunteers (mean ± standard deviation). There was no significant difference seen between the two groups for any of the quantities at a p-value of 0.01

	Patients (n = 16)	Volunteers (n = 8)	p-value
Age (years)	72 ± 8	63 ± 7	—
Heart Rate (bpm)	72 ± 9	79 ± 16	NS
End-diastolic diameter (mm)	6.7 ± 0.9	7.1 ± 0.9	NS
End-systolic diameter (mm)	7.5 ± 1.1	7.8 ± 1.1	NS
Average velocity (cm/sec)	16.9 ± 5.9	17.2 ± 5.1	NS
Mean flow (ml/min)	455 ± 164	381 ± 71	NS
Peak centerline velocity (c/sec)	66 ± 13	69 ± 11	NS
Mean wall shear stress (dynes/cm^2)	7.5 ± 2.5	8.0 ± 4.1	NS

are listed in Table 1. No significant difference between the groups was seen for any of the quantities at a p-value of 0.01.

Determination of wall shear stress

Mean-average WSS (mean ± standard deviation; dynes/cm^2) was 7.5 ± 2.5 for the carotid artery stenosis patients, and 8.0 ± 4.1 for the volunteers. Differences in the WSS values between the patients and volunteers were not significant at a p-value of 0.01. Individual measurements of WSS varied considerably, as is evident from the large standard deviations. The large variation in mean WSS is due in part to the unique flow velocity and vessel geometry of each subject generated by normal biological variation among subjects. This large variation has also been seen in previous studies (19, 27, 28).

Several correlations were performed on the data to test for bias. First, there was no difference in WSS between men and women in either the patients or volunteers (p = 0.6). Second, there was low correlation between WSS and percent stenosis (r = 0.24). Third, there was low correlation between WSS and flow (r = 0.4).

DISCUSSION

MR phase velocity mapping was used to determine mean-average WSS values in the common carotid arteries of patients with carotid bifurcation atherosclerosis. The study found that there was no significant difference in mean-average WSS between patients with atherosclerosis and in volunteers of similar ages with no evidence of luminal narrowing.

Gnasso et al. found that WSS was higher in the non-diseased carotid than the diseased carotid in patients with asymmetric carotid artery disease (15). The increased WSS in the non-diseased carotid artery found in their study may be due to decreased flow resistance causing a higher velocity and hence a higher WSS (eq. 1). The diseased versus non-diseased differences in WSS within a patient may be an effect of the stenosis rather than a cause of the stenosis. By eliminating patients with asymmetric disease and measuring WSS in patients with bilateral luminal narrowing, the effect of asymmetric resistance differences within a subject was mitigated in our study. Our data show that mean-average WSS values are not significantly different in the common carotid artery in patients with carotid bifurcation atherosclerosis and volunteers with no disease. Hence, mean average WSS in the common carotid artery cannot be used to predict disease in the carotid bifurcation.

The reason measuring WSS in the common carotid upstream of a bifurcation does not correlate with disease may be related to the effect of geometry on the flow patterns. Flow in the common carotid artery is laminar and well-behaved, yet flow in the carotid bifurcation can be extremely complex due to the divergent geometry—even in healthy volunteers without evidence of disease. Large variations in both the temporal and spatial location of WSS patterns occur in the carotid bulb, despite the well-behaved nature of flow in the common carotid artery. The flow patterns in the carotid bifurcation are due to the geometry and time-varying nature of the flow and are almost independent

of the mean-average flow in the common carotid artery (10, 11). The specific vessel geometry at the bifurcation and the time-dependent pulsatility of the flow will affect the formation of these low WSS regions.

WSS is important in the development of atherosclerosis, and several groups, including ours, have shown this is due to its effect on a very localized level (29, 30). Atherosclerosis tends to form at branch points, bifurcations, and on the inner walls of curving vessels, such as the carotid bifurcation (9, 10, 31, 32). Prior to the formation of an atherosclerotic lesion, these localized areas have been associated with low and/or oscillating WSS. The determination of WSS in these localized areas cannot be determined using eq. 1, as this method yields a WSS value averaged around an entire vessel cross-section, which necessarily averages out any local differences around the wall. It is difficult to reach conclusions about the cause and effect relationship of WSS and the distribution of atherosclerosis using an equation that averages out local geometric variations of WSS.

Several methods to determine circumferentially-localized, time-dependant, *in vivo* WSS measurements have been proposed. These methods fall into three major methodologies: 1) direct WSS calculation based on MRI velocity measurements (19, 27, 29, 36); 2) combining bi-planar x-ray angiography and intravascular ultrasound-based geometry and flow measurements (37); 3) combining MRI flow and geometry measurements with computation fluid dynamics (CFD) (38, 39). However, all of these methods are both time-consuming and computationally-intensive.

Although mean average WSS may not vary between patients with disease and volunteers, there is strong evidence to suggest that adaptation of vessel diameter to changing flow conditions may be regulated by the mean-average WSS (12, 13). A value of 15 dynes/cm^2 has often been quoted as a mean-average WSS value to which vessels will normalize by changing diameter in response to changing flow conditions. However, recent studies measuring WSS in humans suggest that this value, which was determined from animal studies, may not be applicable in a wide range of human vessels (14, 27, 28). Our current study suggests that mean-average WSS is closer to 8 dynes/cm^2 in the carotid arteries of elderly subjects. Mean-average WSS values found in both normal subjects and patients with bilateral disease fit with the vessel adaptation theory, but with a WSS value lower than is customarily quoted.

In addition to the previously mentioned limitation that eq. 1 determines a spatially and temporally averaged WSS value, the equation makes other assumptions. The equation assumes rigid walls. However, the effect of compliance on the mean WSS is small (34). The equation also assumes that blood is a Newtonian fluid, that is, a fluid where viscosity is not a function of shear rate. Blood has a fairly constant viscosity value of *3.5–4.5* cPoise at the shear rates expected in-vivo, so the value of 4.0 used in this study is a reasonable assumption for WSS calculations. Equation 1 also assumes that a vessel is circular in cross-section. This is usually not a problem in arteries if measurements are not taken near a bifurcation or in an area of disease, as was the case for measurements in the common carotid artery in our study.

In conclusion, we found no differences in mean-average WSS in the common carotid artery between patients with bilateral carotid bifurcation disease and volunteers with no evidence of carotid bifurcation disease. The development of atherosclerosis is highly localized and thus its relationship to WSS is highly localized. Therefore, this relationship may not be accessible through temporal and spatial averages of WSS.

REFERENCES

1. Levesque MJ, Liepsh D, Moravec S, Nerem RM. Correlation of Endothelial Cell Shape and Wall Shear Stress in a Stenosed Dog Aorta. Arteriosclerosis 1986;6:220–9.
2. Nerem RM, Levesque MJ, Cornhill JF. Vascular Endothelial Morphology as an Indicator of Blood Flow. J Biomech Eng 1981;103:172–6.
3. Gerrity RG, Gross JA, Soby L. Control of monocyte recruitment by chemotactic factors in lesion prone areas of swine aorta. Arteriosclerosis 1985;5:55–6.
4. Sharefkin JB, Diamond SL, Eskin SG, McIntire LV, Dieffenbach CW. Fluid flow decreases preproendohelin mRNA levels and suppresses endothelin-1 peptide release in cultured human endothelial cells. J Vasc Surg 1991;141:1–9.
5. Kuchan MJ, Frangos JA. Shear stress regulates endothelin-1 release via protein kinase C and cGMP in cultured endothelial cells. Am J Physiol 1993;264:H150–6.
6. Olesen SP, Clapham DE, Davies PF. Haemodynamic shear stress activates a K+ current in vascular endothelial cells. Nature 1988;331:168–70.
7. Shen J, Luscinskas FW, Connolly A, Dewey CF Jr. Gimbrone MA Jr. Fluid shear stress modulates cytosolic free calcium in vascular entothelial cells. Am J Physiol 1992;262:0384–90.
8. Nishida K, Harrison DG, Navas JP, Fisher AA, Dockery SP, Uematsu M, Nerem RM, Alexander RW, Murphy TJ. Molecular Cloning and Characterization of the Constituative Bovine Endothelial Cell Nitric Oxide Synthase. J Clin Invest 1992;90:2092–96.
9. Caro CG, Fitzgerald JM, Schoter RC. Atheroma and Arterial Wall Shear. Observation, Correlation, and a Proposal of a Shear Dependent Mass Transfer Mechanism for Atherogenesis. Proc Royal Soc London B 1971;177:109–59.
10. Ku DN, Giddens DP, Zarins CK, Glagov S. Pulsatile Flow and Atherosclerosis in the Human Carotid Bifurcation. Arteriosclerosis 1985;5:293–302.
11. Friedman MH, Hutchins GM, Bargeron CB, Deters DJ, Mark FF. Correlation Between Intimal Thickness and Fluid Shear in Human Arteries. Atherosclerosis 1981;39:425–36.
12. Zarins CK, Zatina MA, Giddens DP, Ku DN, Glagov S. Shear stress regulation of artery lumen diameter in experimental atherogenesis. J Vase Surg 1987;5:413–20.
13. Kamiya A, Togawa T. Adaptive Regulation of Wall Shear Stress to Flow Change in the Canine Carotid Artery. Am J Physiol 1980;H14–H21.
14. Gnasso A, Carallo C, Irace C, Spagnuolo V, De Novara G, Mattioli PK, Pujia A. Association between intima-media thickness and wall shear stress in the common carotid arteries in healthy male subjects. Circulation 1996;94:3257–62.
15. Gnasso A, Carallo C, Irace C, Spagnuolo V, De Novara G, Mattioli PK, Pujia A. In-vivo association between low wall shear stress and plaque in subjects with asymmetrical carotid arteriosclerosis. Stroke 1997;28:993–8.
16. Eliasziw M, Smith RF, Singh N, Holdsworth DW, Fox AJ, Barnett H. Further comments on the measurement of carotid stenosis from angiograms. North American Symptomatic Carotid Endarterectomy Trial (NASCET) Group. Stroke 1994 Dec;25(12):2445–9.

17. Oshinski JN, Pettigrew RI, and Ku DN. Turbulent Fluctuation Velocity: The Most Significant Determinate in Post-stenotic Signal Loss. Mag Res Med 1995:33:193–9.

18. Firmin DN, Nayler GL, Kilner PJ, Longmore DB. The Application of Phase Shifts in NMR for Flow Measurements. Mag Res Mec 1990;14:230–41.

19. Oshinski JN, Ku DN, Mukundan S, Loth F, Pettigrew RI. Determination of Wall Shear Stress in the Aorta with the Use of MR Phase Velocity Mapping. J Mag Res Imag 1995;5:640–7.

20. Chatzimavroudis GP, Walker PG, Oshinski JN, Franch RH, Pettigrew RI, Yoganathan AP. The importance of slice location on the accuracy of aortic regurgitation measurements with magnetic resonance phase velocity mapping. Ann Biomed Eng 1997 Jul-Aug; 25(4):644–52.

21. van der Geest RJ, Jansen E, Buller WGM, Reiber JHC. Comparison between manual and semiautomated analysis of left ventricular volume parameters from short-axis MR images. J Comput Assist Tomogr 1997;21:756–6.

22. Fung YC. Biomechanics. Springer-Verlag, New York, 1981, p. 63.

23. Hulley SB, Cummings SR, Browner WS, Grady D, Hearst N, Newman TB. Designing Clinical Research. Lippincott Williams, Philadelphia, PA, 2001, pp. 65–85.

24. Womersley JR. Elastic Tube Theory of Pulse Transmission and Oscillatory Flow in Mammalian Arteries. Technical Report WADC-TR 56-614. 1957. Wright Air Development Center, Dayton, OH.

25. Lieber BB and Giddens DP. Post-Stenotic Core Flow Behavior in Pulsatile Flow and its Effects on Wall Shear Stress. J Biomechanics. 1990;23:597–605.

26. Young DF. Fluid Mechanics of Arterial Stenoses. J Biomechan Eng 1979;101:157.

27. Oyre S, Pedersen EM, Ringgaard S, Boesiger P, Paaske WP. In vivo wall shear stress measured by magnetic resonance velocity mapping in the normal human abdominal aorta. Eur J Vasc Endovasc Surg 1997; 13(3):263–71.

28. Samijo SK, Willigers JM, Barkhuysen R, Kitslaar PJ, Reneman RS, Hoeks AP, Wall shear stress in the human common carotid artery as a function of age and gender. Cardvasc Res 1998;39: 515–22.

29. Cheng CP, Herfkens RJ, Taylor CA. Comparison of abdominal aortic hemodynamics between men and women at rest and during lower limb exercise. J Vasc Surg 2003;37:118–23.

29. Loth F, Jones SA, Giddens DP, Bassiouny HS, Glagov S, Zarins CK. Measurements of velocity and wall shear stress inside a PTFE vascular graft model under steady flow conditions. J Biomech Eng, 1997;119:187–94.

30. Jin S, Oshinski J, Giddens DP. Effects of wall motion and compliance on flow patterns in the ascending aorta. J Biomech Eng. 2003;125:347–54.

31. Thomas JB, Milner JS, Rutt BK, Steinman DA. Reproducibility of image-based computational fluid dynamics models of the human carotid bifurcation. Ann Biomed Eng 2003;31:132–41.

32. Glagov S, Rowley DA, Kohut RI. Atherosclerosis of Human Aorta and its Coronary Arteries. Arch Path 1961;72:82–95.

33. Glagov S, Ozoa AK. Significance of the relatively Low Incidence of Atherosclerosis in the Pulmonary, Renal, and Mesenteric Arteries. Annals NY Acad Sci 1968;149:940–55.

34. Anayiotos AS, Jones SA, Giddens DP, Glagov S, Zarins CK. Shear Stress in a Compliant Model of the Human Carotid Bifurcation. J Biomech Eng 1994;116:98106.

35. Steinman DA. Image-based computational fluid dynamics modeling in realistic arterial geometries, Ann Biomed Eng 2002;30: 483–97.

36. Frayne R, Rutt B. Measurement of Fluid-Shear Rate by Fourier-Encoded Velocity Imaging. Magn Reson Med 1995;34:378–87.

37. Krams R, Wentzel JJ, Oomen JAF, Binke R, Schuurbiers JCH, de Feyter PJ, Serruys PW, Slager CJ. Evaluation of Endothelial Shear Stress and 3D Geometry as Factors Determining the Development of Atherosclerorsis and Remodeling in Human Coronary Arteries in Vivo. Arteriosclerosis, Thrombosis, and Vascular Biology 1997;17:2061–5.

38. Kaazempur-Mofrad MR, Isasi AG, Younis HF, Chan RC, Hinton DP, Sukhova G, LaMuraglia GM, Lee RT, Kamm RD. Characterization of the atherosclerotic carotid bifurcation using MRI, finite element modeling, and histology. Ann Biomed Eng 2004 Jul;32:932–46.

39. Papathanasoupoulou P, Zhao S, Kohler W, Robertson MB, Long Q, Hoskin P, Xu XY, Marshall I. MRI Measurement of Time-Resolved Wall Shear Stress Vectors in a Carotid Bifurcation Model, and Comparison With CFD Predictions. J Magn Reson Img. 2003;17:153–62.